

***M*-shell ionization of Au, Bi, and U by protons and helium ions in the MeV region**

K. Ishii and S. Morita

Department of Physics, Tohoku University, Sendai, Japan

H. Tawara

Nuclear Engineering Department, Kyushu University, Fukuoka, Japan

H. Kaji and T. Shiokawa

Department of Chemistry, Tohoku University, Sendai, Japan

(Received 15 July 1974)

The *M*-shell x-ray production cross sections in Au, Bi, and U were measured with a Si(Li) detector for proton and ³He-ion bombardments over the energy range 1.0–4.5 MeV and 3.0–9.0 MeV, respectively. Absolute ionization cross sections are derived and compared to the predictions of the binary-encounter approximation (BEA) and the plane-wave Born approximation (PWBA). Systematic deviation of the experimental results from the scaled universal curve of the BEA is found. It is shown that this deviation can be understood by taking into account the velocity distribution function for the 3*d* electrons. Good agreement between the PWBA calculation of Choi and the experimental results is obtained for the *M*-shell ionization of Au. The ratios of the ionization cross sections for proton bombardment to those for helium-ion bombardment, at equal velocities, deviate substantially from the theoretical Z_1^2 dependence and show so-called crossover behavior, which has been found for the *K*- and *L*-shell ionization.

I. INTRODUCTION

In the past several years *K*-shell ionization cross sections have been extensively measured by using collisions of simple heavy charged particles, as are tabulated by Garcia *et al.*¹ and Rutledge and Watson,² and have been interpreted by the plane-wave Born approximation (PWBA), binary-encounter approximation (BEA), and their modifications, giving general agreements with experimental results within an accuracy of 20%. Measurements on the *L*-shell ionization are in progress in various laboratories. Those on the *M*-shell ionization, however, are still very scarce, mainly because of the complex structures of the *M*-shell x-ray lines and also of the large uncertainty of the fluorescence yields and the Coster-Kronig transition probabilities for the *M* shell.

Khan *et al.*³ have measured the *M*-shell x-ray production cross sections of six medium-heavy elements using thick targets. Their results on Ho and Gd are about one order of magnitude smaller than the BEA predictions. Busch *et al.*⁴ measured the *M* x-ray production cross section using a thin Pb target under proton bombardment in the energy range 0.5–14.0 MeV and found that the BEA prediction is systematically about 20% lower than the experimental results and that the BEA curve exhibits a maximum at a proton energy of about 6 MeV, as compared to about 7–8 MeV experimentally. Recently, Choi⁵ has calculated the *M*-shell ionization cross sections for some heavy elements

based on the PWBA using screened hydrogenic wave functions for the atomic electrons and found that the dominant contribution to the total *M*-shell ionization cross section comes from the 3*d* subshell, as the 3*d* subshell is the outermost shell among the *M* subshells.

This work presents the result of a study on the *M* x-ray measurements of Au, Bi, and U targets produced by incident protons and ³He ions over the energy ranges 1.0–4.5 and 3–9 MeV, respectively. The *M*-shell ionization cross sections as a function of the projectile energy are compared to the available theoretical predictions. The ratios of the *M*-shell ionization cross sections for protons to those for ³He ions are also discussed.

II. EXPERIMENT AND RESULTS

The general experimental arrangement has been previously described,⁶ and only details related to this measurement will be discussed. Proton and ³He-ion beams from the 5-MV Van de Graaff accelerator of Tohoku University were used. Gold and bismuth targets of 348 and 431 $\mu\text{g}/\text{cm}^2$, respectively, were prepared by vacuum evaporation of pure metal onto 100- $\mu\text{g}/\text{cm}^2$ Al foils and a uranium target of 291 $\mu\text{g}/\text{cm}^2$ was prepared by electro-spraying a solution of $(\text{CH}_3\text{COO})_2\text{UO}_2 \cdot 2\text{H}_2\text{O}$ on an Al backing of 100 $\mu\text{g}/\text{cm}^2$. The thickness of these targets was measured by the Rutherford scattering of

3.5-MeV protons. An Ortec Si(Li) detector, located at an angle of 90° with respect to the incident beam, had a resolution of 205 eV at 6 keV, an effective area of 30.0 mm^2 , and a 0.001-in.-thick Be window. The x rays passed through a Mylar vacuum-chamber window of $10 \mu\text{m}$ and an air path of 50.4 and 26.0 mm for proton and ^3He -ion experiments, respectively, before entering the detector. In order to monitor possible target deterioration during the bombardment, elastically scattered particles were measured with a solid state detector simultaneously. The counting rate was kept below 100 cps to avoid a piling-up effect.

Sample spectra obtained are presented in Fig. 1. The major M peak is composed of unresolved $M\alpha$ and $M\beta$ lines, which result from vacancies in the M_4 and M_5 subshells. The observed x-ray yields Y_M were converted to the x-ray production cross sections by the formula

$$\sigma_M^X = 4\pi Y_M / A_M \epsilon_M \phi N \Delta\Omega, \quad (1)$$

where the angular distribution of M x rays is assumed to be isotropic, A_M is the correction factor of the x-ray absorption in the target, the Mylar window, and air path, ϵ_M is the relative detection efficiency for each x ray, ϕ is the number of particles incident on the target, N is the number of target atoms per cm^2 , and $\Delta\Omega$ is the solid angle subtended by the x-ray detector. The absorption in the Mylar window and the air path was measured experimentally and the differences in A_M and ϵ_M for the two main M x-ray peaks of the spectra were taken into account.

Experimental uncertainties for each of the data points include those of (a) detection efficiency (10%), (b) target thickness (<7%), (c) the target-to-detector absorption (5%) and (d) background subtraction (3%). The uncertainties due to counting statistics are negligible. Since the largest contributions are from the target thickness and detection efficiency, the relative error from point to point is considerably smaller than indicated. The experimental M x-ray production cross sections thus obtained for proton and ^3He -ion bombardments are presented in Fig. 2. It must be noted that the slope of these excitation curves for proton bombardment is evidently different from that for helium-ion bombardment.

III. DISCUSSION

The total x-ray production cross section σ_M^X is related to the M -subshell ionization cross section $\sigma_{M_k}^i$ of the k th subshell of the M shell by

$$\sigma_M^X = \sum_{k=1}^5 \omega_k^{\text{eff}} \sigma_{M_k}^i, \quad (2)$$

where ω_k^{eff} is the effective fluorescence yield of the k th subshell, taking into account the Coster-Kronig yields. Assuming that all subshell ionization cross sections per electron in the subshell are equal; that is, $\sigma_{M_k}^i = (N_k/18)\sigma_M^i$, where σ_M^i is the total M -shell ionization cross section and N_k is the number of

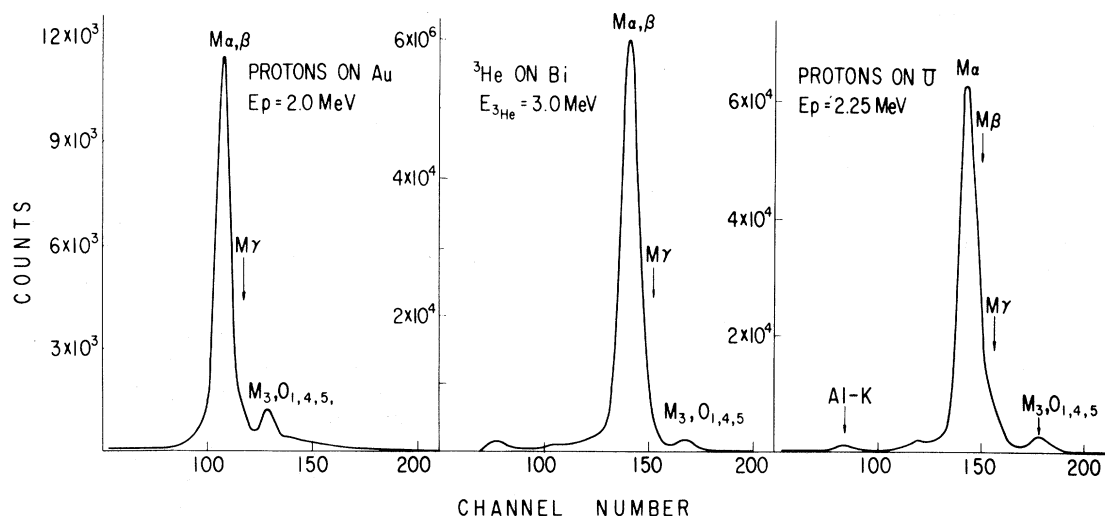


FIG. 1. M x-ray spectra of Au, Bi, and U produced by proton or helium-ion bombardment.

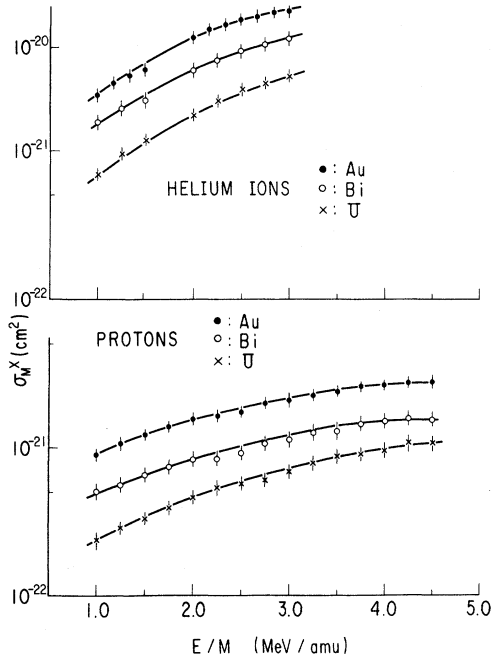


FIG. 2. Experimental M -shell x-ray production cross sections for Au, Bi, and U as a function of projectile energy.

electrons in the k th subshell, we obtain

$$\sigma_M^X \approx \bar{\omega}_M \sigma_M^i, \text{ or } \sigma_M^i \approx \sigma_M^X / \bar{\omega}_M. \quad (3)$$

Here $\bar{\omega}_M$ is the average fluorescence yield of the M -shell given as:

$$\bar{\omega}_M = \sum_{k=1}^5 \omega_k^{\text{eff}} N_k / 18. \quad (4)$$

The values of ω_M are taken from papers of Bambynek *et al.*⁷ and Baker *et al.*⁸ as 0.023, 0.035, and 0.045 for Au, Bi, and U, respectively. Since $\bar{\omega}_M$ depends on the relative probability for producing a vacancy in a given subshell as well as the Coster-Kronig transition yields, the value of $\bar{\omega}_M$ may depend on the nature of the ionization or excitation processes used in its measurement. For this reason the theoretical value of σ_M^i may be expected to deviate systematically from the experimental values determined from the x-ray measurements.

A. BEA

The electron-velocity distributions for the $1s$, $2p$, and $3d$ shells were calculated using the momentum representation of the hydrogenic wave functions,

$$\rho_{1s}(v) dv = (32/\pi) v_0^5 [v^2 / (v_0^2 + v^2)^4] dv, \quad (5)$$

$$\rho_{2p}(v) dv = (2 \times 4^4 / 3\pi) v_0^7 [v^4 / (v_0^2 + v^2)^6] dv, \quad (6)$$

$$\rho_{3d}(v) dv = (4^6 / 5\pi) v_0^9 [v^6 / (v_0^2 + v^2)^8] dv, \quad (7)$$

where v_0 is given by $U = \frac{1}{2} m_e v_0^2$, U is the binding energy, and m_e is the electron mass. Here U is taken as an average binding energy for the M shell formed by weighting the number of the electrons in the subshell.

The ionization cross section for each shell can be calculated by putting these velocity distributions into the formula given by Garcia,⁹

$$\sigma_{nl}^i = N_{nl} \int_0^\infty \sigma^i(v_1, v) \rho_{nl}(v) dv. \quad (8)$$

Here n and l are the principal and orbital quantum numbers, respectively, v_1 is the velocity of the incident particle, and σ^i is the cross section for removal of an atomic electron whose velocity is v . The calculated ionization cross sections for these shells are shown in Fig. 3. The behavior of the ionization cross section for the $2p$ shell is quite consistent with that obtained from the constrained BEA by Hansen.¹⁰ From this figure, it is found that

$$\sigma_{1s} U_{1s}^2 (Z_1^2 N_{1s})^{-1} > \sigma_{2p} U_{2p}^2 (Z_1^2 N_{2p})^{-1} > \sigma_{3d} U_{3d}^2 (Z_1^2 N_{3d})^{-1}, \quad (9)$$

for $\sim 1.0 > E(\lambda U)^{-1} > 0.25$,

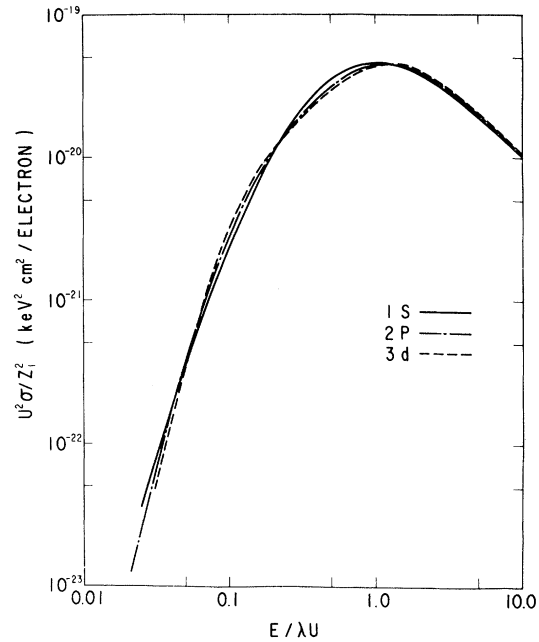


FIG. 3. Scaled ionization cross sections for the $1s$ (solid curve), $2p$ (dash-dot curve), and $3d$ (dashed curve) electrons calculated from the BEA. The maximum cross section for the $1s$ electrons is obtained at $E/\lambda U = 1.0$, while those for the $2p$ and $3d$ electrons are at $E/\lambda U \approx 1.2$.

and

$$\sigma_{3d} U_{3d}^2 (Z_1^2 N_{3d})^{-1} > \sigma_{2p} U_{2p}^2 (Z_1^2 N_{2p})^{-1} > \sigma_{1s} U_{1s}^2 (Z_1^2 N_{1s})^{-1},$$

for $0.25 > E(\lambda U)^{-1} > 0.045$, (10)

where Z_1 is the nuclear charge of the projectile, N is the number of electrons in each shell, E is the energy of the projectile, and $\lambda = 1836.1$ is the mass ratio of proton to electron. The shift of the maximum cross section at about 6 MeV proton energy of the BEA curve to about 7–8 MeV experimentally, reported by Busch *et al.*⁴ on the Pb M -shell ionization, can be understood from Fig. 3.

Figure 4 gives the comparison of our experimental results of the ionization cross section with the scaled BEA curve for K -shell ionization. The results for the Sn K shell and Sn L_3 and Ta L_3 subshells have previously been reported.^{6,11} The ionization cross sections for the Au $M_{4,5}$ subshell were estimated from the measured total M -shell cross sections and ratios of the calculated subshell ionization cross sections to the total ionization cross section calculated by Choi, shown in Fig. 5; that is,

$$(\sigma_{M_{4,5}})_{\text{expt}/2 \text{ elect}} = [(6\sigma_{M_5}^i + 4\sigma_{M_4}^i) / \sigma_M^i] C_{\text{choi}}^{1/5} (\sigma_M^i)_{\text{expt}}, \quad (11)$$

where σ_M^i is the total M -shell ionization cross section and is given by

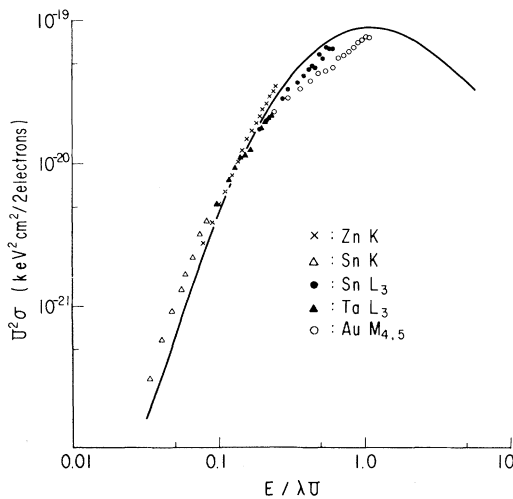


FIG. 4: Comparison of the measured K -, L -, and M -shell ionization cross sections by protons with the scaled BEA curve (solid line) for the K -shell ionization.

$$\sigma_M^i = \sum_{k=1}^5 \sigma_{M_k}^i. \quad (12)$$

It is found from Fig. 4 that the general behavior of the experimental results on the M -shell ionization is quite consistent with the calculation of the BEA, showing the trend of Eq. (9).

B. PWBA

Figures 5 and 6 illustrate the comparison of the measured M -shell ionization cross sections for proton impact on Au and U, respectively, with the predictions of the PWBA calculated by Choi.⁵ The L -shell ionization cross sections, which are also shown for comparison, considering the effect of the Coulomb deflection, are quite consistent with the theoretical predictions and will be discussed in a separate paper. As seen in Fig. 5, the M_4 and M_5 subshells give the dominant contributions to the M -shell ionization. The effect of the Coulomb deflection of the projectile in the field of target nucleus on the M -shell ionization has been estimated from the function $(9E_{10})$ given by Basbas *et al.*¹² and was found to be at most 6% in the present energy region. It must be noted that the agreement between the experimental results and the predictions of the PWBA is quite good. Considering the ambiguity of the fluorescence yields mentioned previously, the lack of absolute agreement in uranium is not surprising.

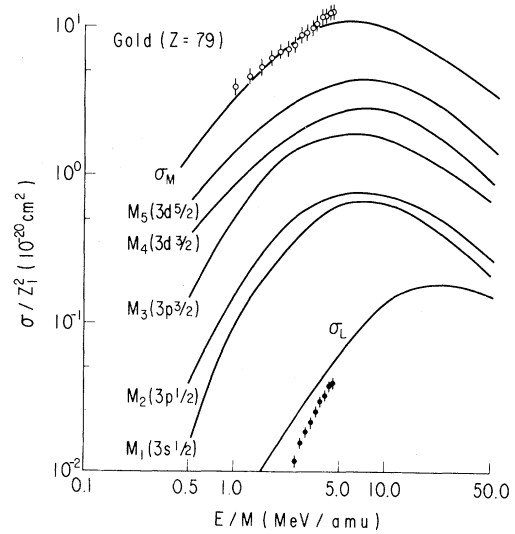


FIG. 5: Comparison of the experimental Au L - and M -shell ionization cross sections with the PWBA calculations of Choi.

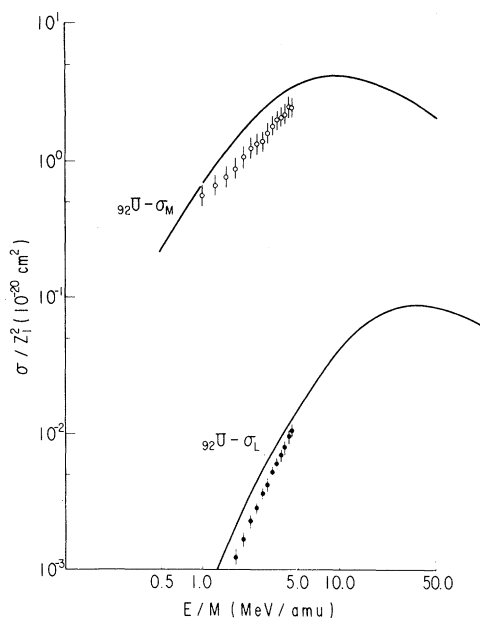


FIG. 6. Comparison of the experimental U L - and M -shell ionization cross sections with the PWBA calculations of Choi.

C. Projectile charge dependence of ionization cross sections

As is well known, both the PWBA and BEA calculations predict the Z_1^2 dependence of ionization cross sections. However, substantial deviation from the Z_1^2 dependence or a crossover behavior has been found for the K -shell ionization of medium elements by Basbas *et al.*¹³ and Lewis *et al.*,¹⁴ and for the L -shell ionization of Pb by Tawara *et al.*⁶ For the case of the K -shell ionization Basbas *et al.*^{13,15} have tried to explain this behavior in terms of the distortion of the shell in the field of the projectile and the Coulomb deflection of the projectile in the field of the target nucleus; meanwhile, Doolen *et al.*¹⁶ and Harrison *et al.*¹⁷ have pointed out the contribution of charge-exchange processes to the inner-shell ionization.

The present experimental results on the ratio of the M -shell ionization cross sections in Au, Bi, and U for protons to those for ^3He ions with equal velocities are shown in Fig. 7, where a crossover behavior is also found for the M -shell ionization in the present bombarding-energy region. The in-

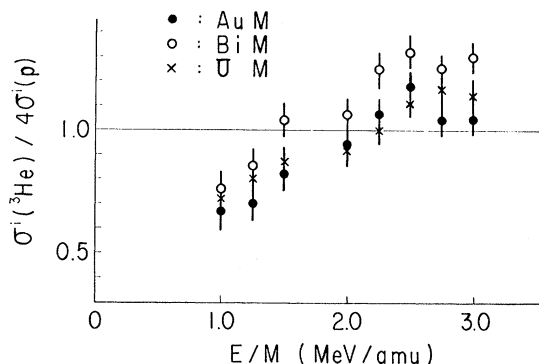


FIG. 7. Ratios of the ionization cross sections by protons to those by ^3He ions with equal velocities.

terpretation of this behavior will be discussed in a separate paper together with our experimental results on the L -shell ionization of these elements.

VI. SUMMARY

The M x-ray yields from thin Au, Bi, and U targets have been measured by proton bombardment over the energy range 1.0–4.5 MeV and by ^3He -ion bombardment over 3.0–9.0 MeV. Though the values of fluorescence yield for the M shell of these elements have rather large uncertainties, the absolute ionization cross sections were estimated from the measured x-ray production cross sections. Based on the scaled BEA, the ionization cross sections for the $2p$ - and $3d$ -shell electrons were calculated and are compared with the experimental results. General behavior and the shift of maximum cross section to higher bombarding energy are consistent with the experiments. Theoretical PWBA calculations by Choi for the M -shell ionization of Au and U are in good agreement with the present results, except for the absolute values of the cross section for uranium. The ratios of the M -shell ionization cross sections by protons to those by helium ions, at equal velocities, show pronounced deviations from the theoretical Z_1^2 dependence.

ACKNOWLEDGMENT

The authors would like to thank M. Kato for his skillful operation of the accelerator during the course of this experiment.

¹J. D. Garcia, R. J. Fortner, and T. M. Kavanagh, *Rev. Mod. Phys.* **45**, 111 (1973).

²C. H. Rutledge and R. L. Watson, *At. Data Nucl. Data Tables* **12**, 195 (1973).

³J. M. Khan, D. L. Potter, and R. D. Worley, *Phys.*

Rev. **139**, A1735 (1965).

⁴C. E. Busch, A. B. Baskin, P. H. Nettles, S. M. Shafron, and A. W. Waltner, *Phys. Rev. A* **7**, 1601 (1973).

⁵Byung-ho Choi, *Phys. Rev. A* **7**, 2056 (1973).

⁶H. Tawara, K. Ishii, S. Morita, H. Kaji, C. N. Shu,

- and T. Shiokawa, *Phys. Rev. A* 9, 1617 (1974).
- ⁷W. Bambynek, B. Crasemann, R. W. Fink, H. U. Freund, H. Mark, C. D. Swift, R. E. Price, and P. V. Rao, *Rev. Mod. Phys.* 44, 716 (1972).
- ⁸K. R. Baker, F. Tolea, R. W. Fink, and J. J. Pinajian, *Bull. Am. Phys. Soc.* 18, 1576 (1973).
- ⁹J. D. Garcia, *Phys. Rev. A* 1, 280 (1970).
- ¹⁰J. S. Hansen, *Phys. Rev. A* 8, 822 (1973).
- ¹¹K. Ishii, S. Morita, H. Tawara, H. Kaji, and T. Shiokawa, *Phys. Rev. A* 10, 774 (1974).
- ¹²G. Basbas, W. Brandt, and R. Laubert, *Phys. Rev. A* 7, 987 (1973).
- ¹³G. Basbas, W. Brandt, R. Laubert, and A. Ratkowski, *Phys. Rev. Lett.* 27, 171 (1971).
- ¹⁴C. W. Lewis, R. L. Watson, and J. B. Natowitz, *Phys. Rev. A* 5, 1773 (1972).
- ¹⁵C. Basbas, W. Brandt, and R. Laubert, *Phys. Lett.* 34A, 227 (1971).
- ¹⁶G. D. Doolen, J. H. McGuire, and M. H. Mittleman, *Phys. Rev. A* 7, 1800 (1973).
- ¹⁷K. G. Harrison, H. Tawara, and F. J. de Heer, *Physica (Utr.)* 66, 16 (1973).